



N7433589

MEMBRANE WATER DEAERATOR INVESTIGATION

AIRESEARCH MFG. CO., LOS ANGELES, CALIF

26 FEB 1974

N7433589



NASA CR-

140259

MEMBRANE WATER DEAERATOR INVESTIGATION

(TASK ORDER NO. 179)


REPORT NO. 74-10072

February 26, 1974

PREPARED BY:

J. Elam
J. Ruder
H. Strumpf

APPROVED BY:


J. M. Ruder
Senior Engineering Specialist



GARRETT RESEARCH MANUFACTURING COMPANY
OF CALIFORNIA

REPRODUCED BY:
U.S. Department of Commerce
National Technical Information Service
Springfield, Virginia 22161

NTIS

CONTENTS

<u>Section</u>		<u>Page</u>
1	PROGRAM SUMMARY	1-1
	Purpose	1-1
	Scope	1-2
	Introduction	1-3
	Summary of Results	1-5
	Recommendations	1-8
2	MEMBRANE TEST PROGRAM	2-1
	Introduction	2-1
	Test System Description	2-4
	Test Results	2-8
3	MEMBRANE PERFORMANCE ANALYSIS	3-1
	Introduction	3-1
	Performance of Test Unit	3-4
	Flight Unit	3-7



ILLUSTRATIONS

<u>Figure</u>		<u>Page</u>
1-1	Membrane Unit Configuration	1-4
1-2	Water Deaerator	1-6
1-3	Predicted Performance of Flight Unit	1-7
2-1	Deaerator Test Setup	2-3
2-2	Membrane Water Deaerator Test Setup	2-5
3-1	Water Deaerator	3-11
3-2	Predicted Performance of Flight Unit	3-12
3-3	Effect of Flow Rate	3-14



TABLES

<u>Table</u>		<u>Page</u>
1-1	Deaerator Problem Statement	1-5
1-2	Deaerator Unit Characteristics	1-5
2-1	Fiber Permeability and Strength Characteristics	2-2
2-2	Test Setup Component Description	2-6
2-3	Membrane Water Deaerator Test Results	2-9
3-1	Deaerator Problem Statement	3-7



SECTION I
PROGRAM SUMMARY

PURPOSE

The purpose of the membrane water deaerator program (Task Order No. 179) was to develop data on a breadboard hollow fiber membrane unit that would remove both dissolved and evolved gas from a water transfer system in order to: (1) assure a hard fill of the EVLSS expendable water tank, (2) prevent flow blockage by gas bubbles in circulating systems, and (3) prevent pump cavitation.



SCOPE

The membrane water deaerator program consisted of three tasks. First, an analytical model to describe the mass transfer of dissolved gas through the bulk liquid and then through the membrane wall was developed. Then a hollow fiber membrane unit was tested to determine its deaeration characteristics. Finally, a configuration for a flight unit meeting a specific problem statement was evaluated. By direction of NASA, testing was halted after a few data points were obtained which proved out the basic concept.



INTRODUCTION

Semi-permeable membranes are thin solid films through which different molecular species diffuse at different rates. Thus, they are potentially applicable to many different mass transfer separation processes as well as phase separation processes in zero-g. Previously, these membranes were fabricated in flat sheets; the flat sheets presented a major obstacle to the full utilization of semi-permeable membranes. A large amount of structure is required to hold flat membranes and a seal is required around both sides of each flat sheet. In addition, each sheet must be supported in order to maintain even a moderate pressure differential (or driving force) across the flat, thin surface.

Recently, semi-permeable membranes have been developed in the form of very small (30 to 250 microns) hollow fibers. These hollow fibers are essentially tubes and, because of their small diameter to thickness ratio, can withstand relatively high pressures. This configuration solves the flat sheet problem of supporting high differential pressures across thin films. A large number of these tubes can be epoxied together at each end of the flow length. Finally, the hollow fibers and epoxied ends are inserted into a metal or polymeric tube, which contains manifolds at each end and an exit port along the tube. The final conceptualized configuration, shown in Figure 1-1, is similar to a single pass tube and shell heat exchanger. Thus, with the emergence of a technique to make hollow fiber type semi-permeable membranes, a lightweight unit can be designed to withstand high pressures and yield higher mass transfer areas than are obtainable with flat sheet membranes. This hollow fiber type of unit is the one used in the current program.

Referring to Figure 1-1, water containing dissolved and/or evolved gas enters the water plenum and flows through the hollow fiber. During passage down the length of the tube, the gases permeate through the membrane due to the gas partial pressure difference between the inside and outside surface of the membrane. The dissolved gas flows out to space vacuum and the water continues down the tube and flows out of the unit, deaerated.



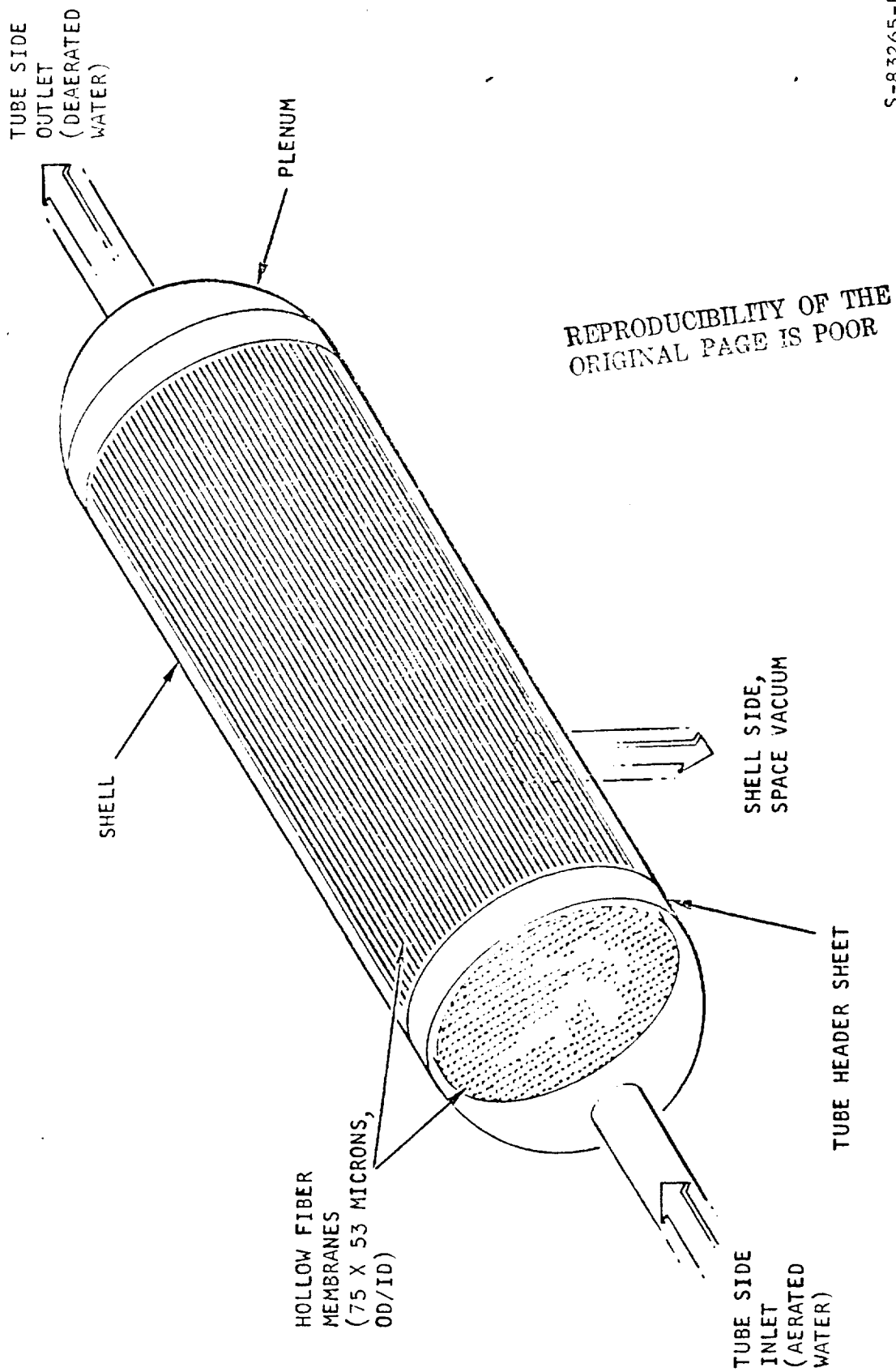


Figure 1-1. Membrane Unit Configuration

SUMMARY OF RESULTS

Using the mathematical model of the deaeration process, a preliminary design was made of a unit that would meet the following problem statement, based on obtaining a hard fill of the expendable EVLSS water tank during servicing.

TABLE 1-1

DEAERATOR PROBLEM STATEMENT

Water Flow Rate	54 lb/hr
Total Pressure	50 psia
Water Temperature	40 to 90°F
Water Side ΔP	5 psi
Dissolved Gas	
In	Saturated with nitrogen at 50 psia
Out	Saturated with nitrogen at 3 psia (max)

The unit to meet the problem statement is shown in Figure 1-2. The design is based on the mathematical model and the test data obtained in the subject program. It is possible that an improved design would result by having the water flow across the tubes with space vacuum on the tube side. However, data are not available for this configuration at this time, so it was not used.

Some of the characteristics of the unit are given in Table 1-2.

TABLE 1-2

DEAERATOR UNIT CHARACTERISTICS

Membrane Material	polymethyl pentene
Envelope (excluding fittings)	2.25 in. dia x 4.2 in.
Weight	0.62 lb
Active area	11.1 ft ²
Tube size	75 O.D. x 53 I.D., microns

Nitrogen partial pressure as a function of length is shown in Figure 1-3.



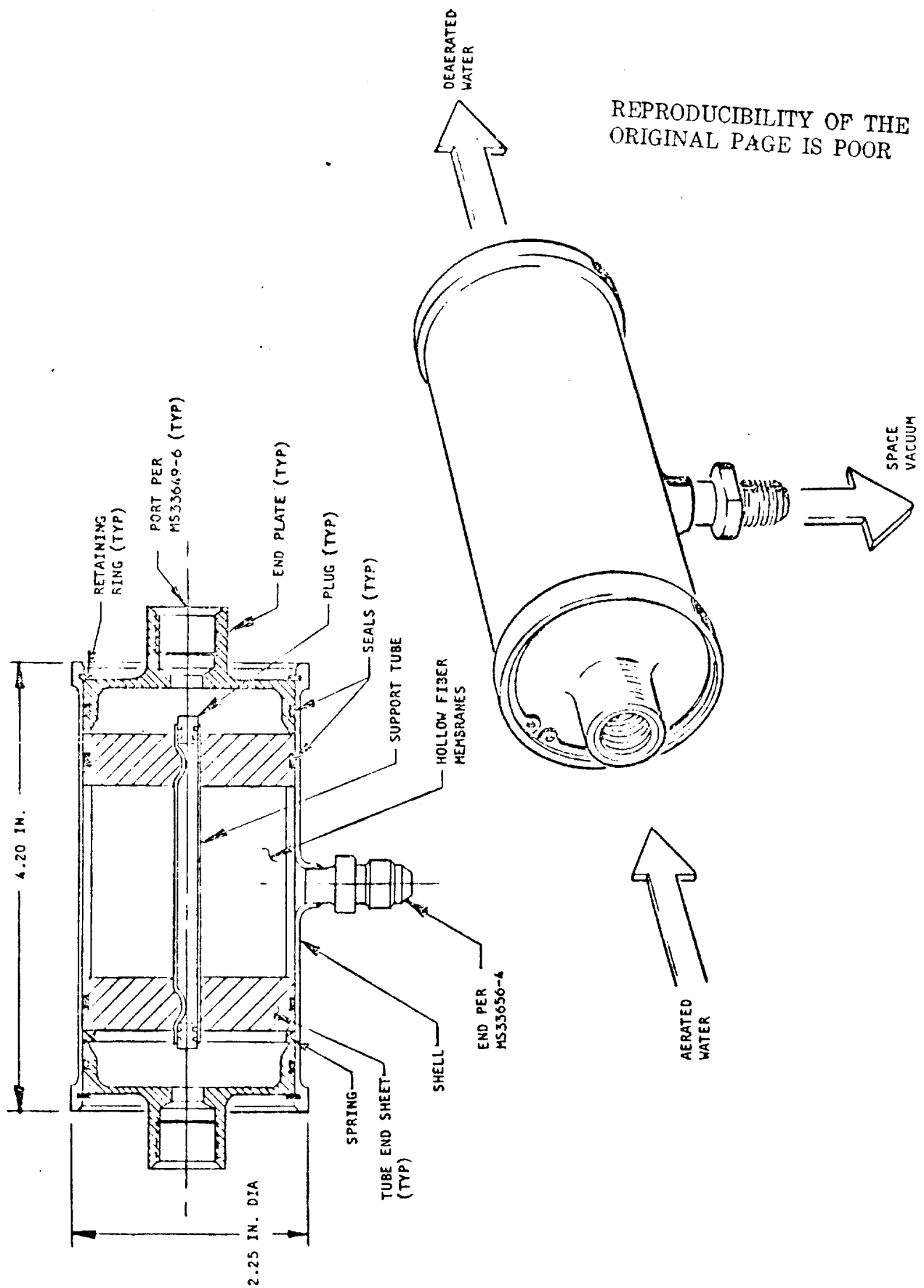


Figure 1-2. Water Deaerator



REPRODUCIBILITY OF THE
ORIGINAL PAGE IS POOR

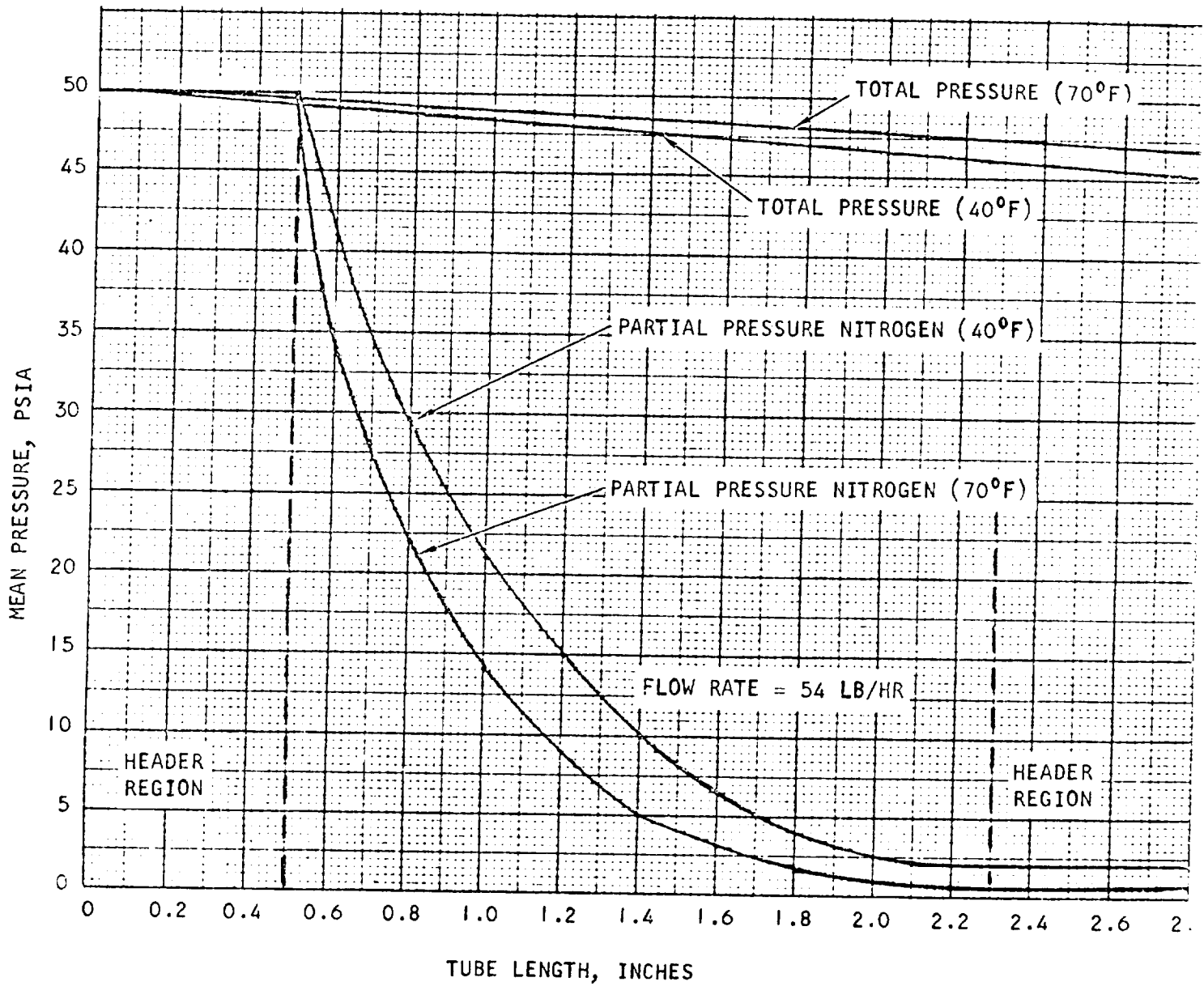


Figure 1-3. Predicted Performance of Flight Unit



AIRSEARCH MANUFACTURING COMPANY
OF CALIFORNIA

RECOMMENDATIONS

The following program plan is recommended for the next phase of work on the membrane deaerator. It is based on the results obtained to date and proposes the development of a unit for a specific EVLSS problem statement.

1. Program Plan

a. Laboratory Tests

Results to date indicate that polymethyl pentene is the best material for the deaerator. Using a laboratory unit, testing will be continued with water flow on the shell side (rather than in the tubes). In addition, three types of tests will be conducted in support of this effort: (1) development of improved techniques to measure dissolved oxygen at low concentrations, (2) determining the effect of a bactericide on the performance of the unit, and (3) determining the strength characteristics of the fiber and the tube end sheet.

b. Analysis and Design

Analyses will be performed to evaluate the data obtained with the laboratory unit. This will then be used to design a unit to a specific problem statement.

c. Fabrication and Verification Tests

A unit will be fabricated and tested to verify its performance. Testing will include the effect of temperature, flow rate, total pressure and dissolved oxygen pressure. In addition, a vibration test will be conducted to verify the integrity of the unit.

d. Documentation

Results of the analytical, design and test effort will be documented in a Final Report. In addition, recommendations will be made for the follow-on effort leading to a qualified unit.



SECTION 2

MEMBRANE TEST PROGRAM

INTRODUCTION

A number of possible hollow fiber materials were evaluated; for the deaerator requirement the most promising material is polymethyl pentene. The selection of polymethyl pentene is based on the fact that (1) the material is a tough plastic that is spinnable into hollow fibers; (2) the permeation rate for the water vapor is low and (3) the permeation rate for oxygen and nitrogen is high. As seen in Table 2-1, the permeability of polymethyl pentene to oxygen and nitrogen is the highest of the presently used membrane fiber materials. Silicone rubber type materials do have a higher permeability, however since the strength of silicone rubber is very low, the advantage of a higher absolute permeability rate is lost when an actual design is made (allowable loop stress for silicone rubber is about one-tenth that of polymethyl pentene).

An available hollow fiber membrane unit made of polymethyl pentene was evaluated as a deaerator. The characteristics of the unit were:

Membrane Material	polymethyl pentene
Tube size	75 O.D. x 53 I.D., microns
Actual surface area	12.2 ft ²
No. of fibers	16,000
Total tube length	15 inches

This available laboratory unit could withstand only a pressure differential of 17 psi across the tube end sheet due to the limited amount of epoxy used in the unit. (The tubes themselves can withstand several hundred psi.) A special fixture was designed to hold the tube shell and water plenum chamber; the original polycarbonate plenum that was made for the unit was not leak tight. The test unit and test setup are shown in Figure 2-1 outside of the vacuum bell jar.



TABLE 2-1
FIBER PERMEABILITY AND STRENGTH CHARACTERISTICS

Material	Permeability (*) at 25°C		Tensile Strength at Yield psi	Elongation at Yield percent
	O ₂	N ₂		
Cellulose	0.0012-0.03 ⁽¹⁾	0.003-0.0096 ⁽¹⁾	---	---
Cellulose acetate	0.4-0.78 ⁽²⁾	0.16-0.5 ⁽²⁾	---	---
Polymethyl pentene	27 ⁽³⁾	6.5 ⁽³⁾	4×10^3 ⁽³⁾	2 ⁽³⁾
Polyethylene terephthalate	0.03 ⁽²⁾	0.005 ⁽²⁾	1.3×10^4 ⁽⁴⁾	3-4 ⁽⁴⁾

*Units (cm³ (STP)-cm/cm²-sec-cm Hg) x 10¹⁰

- (1) 1971-1972 Modern Plastics Encyclopedia, p. 622
- (2) A. Lebovits, Modern Plastics, 43, 139 (1966)
- (3) International Chemical Industries, Technical Bulletin, No. 252
- (4) L. Amborsk and D. W. Flier, Industrial and Engineering Chemistry 45, 2290 (1953)



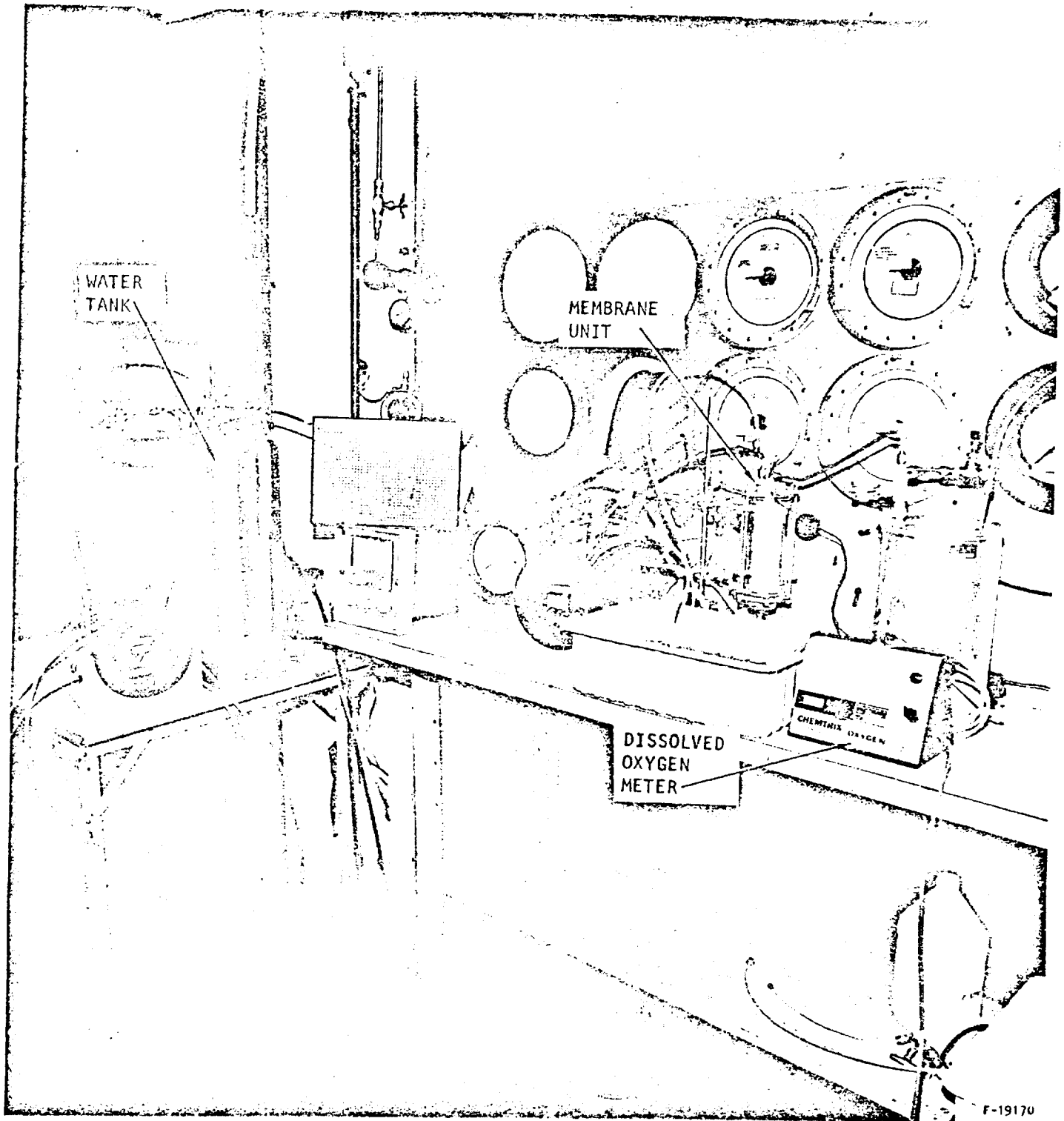


Figure 2-1. Deaerator Test Setup



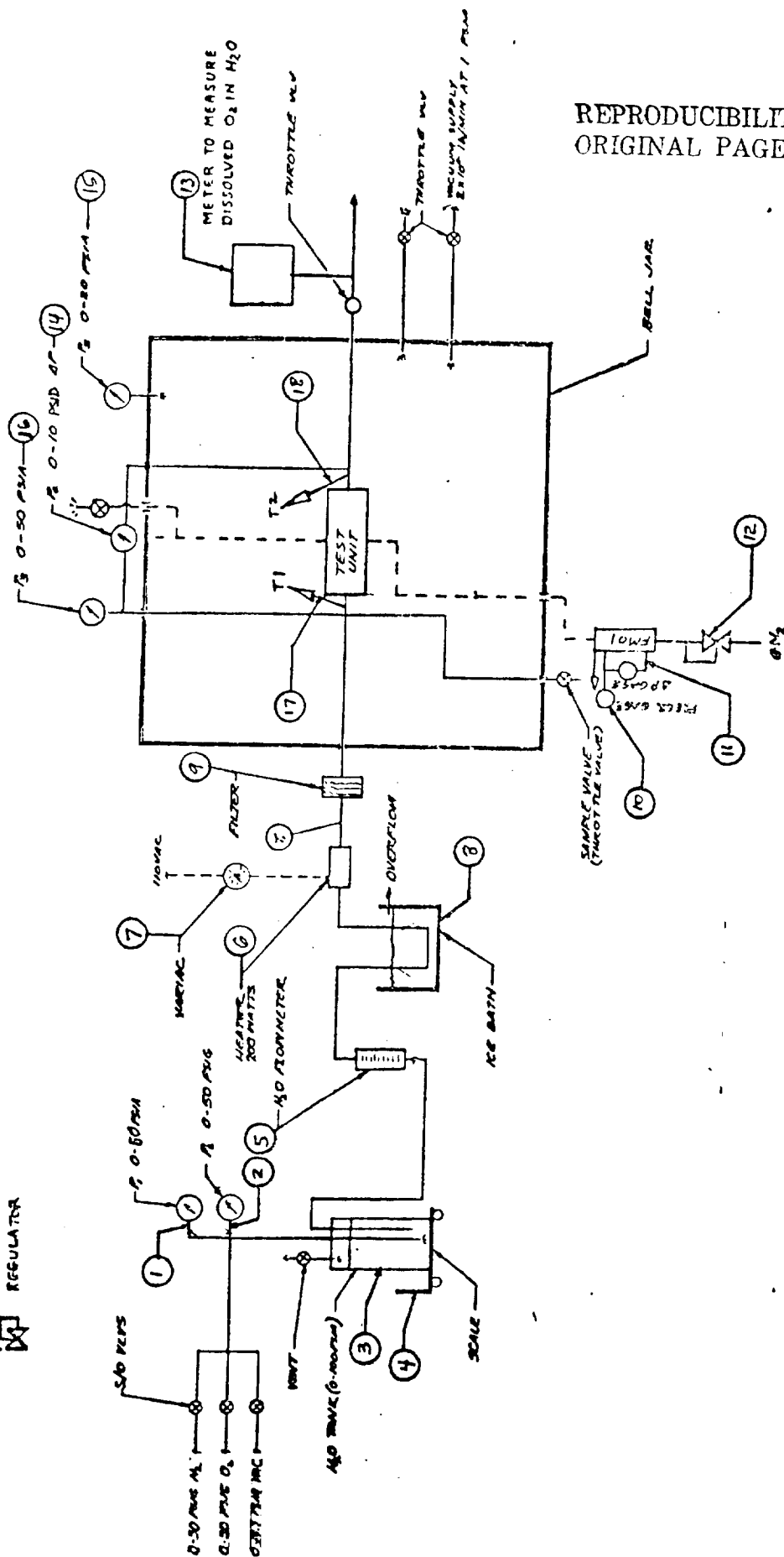
TEST SYSTEM DESCRIPTION

The purpose of the deaerator test program was to obtain data on the mass transfer rate of dissolved oxygen through the bulk fluid and membrane wall of a semi-permeable hollow fiber membrane unit. Oxygen was used as the test fluid because it can more easily be measured, than nitrogen, when dissolved in water. Based on the known permeability values of oxygen and nitrogen (Table 2-1) the performance with nitrogen can be determined. This was done, as shown in Figure 2-2, by saturating a tank containing water, with oxygen. The oxygenated water then flows through the tube side of the test unit. On the shell side, a low oxygen partial pressure is created by either pulling a vacuum or purging with nitrogen. Dissolved oxygen quantity in the water tank is verified by using a laboratory aerometer. Oxygen concentration from the outlet of the unit was measured by an electrochemical dissolved oxygen sensor. The test setup components, shown in Figure 2-2, are described in Table 2-2.





⊗ SHUTOFF VALVE
↑ THERMOCOUPLE
REGULATOR



REPRODUCIBILITY OF THE
ORIGINAL PAGE IS POOR

Figure 2-2. Membrane Water Deaerator Test Setup

TABLE 2-2

TEST SETUP COMPONENT DESCRIPTIONS

ITEM NO.	COMPONENT	DESCRIPTION
1	Pressure Gage	Measures absolute water tank pressure. Range 0 - 50 psia, accuracy $\pm 0.5\%$ full scale.
2	Pressure Gage	Measures gage water pressure. Range 0 - 50 psig, accuracy $\pm 0.5\%$ full scale.
3	Water tank	Provides a water reservoir. Capacity, seven gallons.
4	Scales	Measures weight of water present in tank. Capacity 0 - 100 lbs, accuracy ± 0.01 lb.
5	Water Flowmeter	Measures water flowrate to inlet of test unit. Range 0 - 30 lb/hr, accuracy $\pm 0.5\%$ of full scale.
6	Water Heater	Supplies heat to water to inlet of test unit. Capacity 200 watts.
7	Variac	Supplies power to control temperature of water to inlet of test unit.
8	Ice Bath	Used to cool water.
9	Filter	Four micron filter (absolute) to remove water contaminants.
10	Pressure Gage	Measures sweep gas flowmeter outlet pressure. Range 0 - 50 psia, accuracy $\pm 0.5\%$ at full scale.
11	ΔP Press. Gage	Measures sweep gas flowmeter ΔP . Range 0 - 10 in. H ₂ O, accuracy $\pm 0.5\%$ full scale.
12	Regulator	Controls inlet pressure to test unit sweep port. Range 0 - 5 psig.



TABLE 2-2 (Continued)

ITEM NO.	COMPONENT	DESCRIPTION
13	Meter	Meter to measure dissolved oxygen concentration in water. Range 0-15 ppm. Accuracy ± 0.2 ppm.
14	ΔP Press. Gage	Measures pressure differential across test unit. Range 0 - 10 psid, accuracy $\pm 0.5\%$ of full scale.
15	Pressure Gage	Measures absolute pressure inside bell jar. Range 0 - 20 psia, accuracy $\pm 0.5\%$ of full scale.
16	Pressure Gage	Measures inlet pressure to test unit. Range 0 - 50 psia, accuracy $\pm 0.5\%$ full scale.
17	Thermocouple (T1)	Measures inlet water temperature to test unit. Range 0 - 130°F, accuracy $\pm 1^\circ\text{F}$.
18	Thermocouple (T2)	Measures outlet water temperature from test unit. Range 0 - 130°F, accuracy $\pm 1^\circ\text{F}$.



TEST RESULTS

Test data obtained from the test setup shown in Figure 2-2, is given in Table 2-3. Three series of tests were run; with nitrogen purge through the shell, with air purge through the shell and under vacuum. Since the unit could only withstand 17 psi differential across the tube sheet, the first test was conducted with nitrogen purge. This resulted in a 17 psi maximum differential pressure across the inlet tube sheet, and a water side pressure drop of about 13 psi. The high water side pressure resulted in a maximum flow of 25.7 lb/hr. At this flow, the unit outlet oxygen partial pressure was still close to zero (actually 0.11 psia).

Using air, the outlet dissolved oxygen corresponds very closely to the shell side oxygen partial, again indicating that all the theoretical possible oxygen was removed.

Finally, at this point, the vacuum was pulled in the chamber to simulate an actual unit. Due to the tube end sheet structure problem, the inlet pressure had to be reduced, thus reducing the water flow rate. Again, the outlet oxygen partial pressure on the water side closely matched the gaseous partial pressure on the shell side. As will be discussed below, analyses indicated that this would be the case.

After the above preliminary series of test were run, by NASA direction, further testing was halted.



REPRODUCIBILITY OF THE
ORIGINAL PAGE IS POOR

TABLE 2-3

MEMBRANE WATER DEAERATOR
TEST RESULTS

Storage Tank		Unit Conditions						Chamber Pressure, psia	Remarks
Total Pressure, psia	Dissolved Oxygen Partial Pressure, psia	Inlet Pressure, psia	Temp., °F	Water Rate, lb/hr	Pressure Drop, psi	Outlet Dissolved Oxygen, psia	Purge Rate, lb/hr		
29.7	30	27.8	72	25.7	12.6	0.11	10	14.7	Shell purged with nitrogen
29.8	30	28.0	72	19.9	10.0	0.11	10	14.7	Shell purged with nitrogen
29.9	30	28.9	72	9.9	5.0	0.11	10	14.7	Shell purged with nitrogen
29.9	30	27.5	72	4.2	2.1	0.07	10	14.7	Shell purged with nitrogen
29.8	30	26.3	72	21.8	11.1	2.8	10	14.7	Shell purged with air
29.9	30	26.0	72	20.3	10.0	2.8	10	14.7	Shell purged with air
29.9	30	28.1	72	9.9	5.0	2.8	10	14.7	Shell purged with air
29.9	30	29.2	72	4.1	2.0	2.6	10	14.7	Shell purged with air
16.7	16.7-30	16.0	72	2.1	1.3	0.11	--	0.21	No purge flow
16.7	16.7-30	16.7	72	3.6	1.9	0.63	--	3.1	No purge flow



SECTION 3

MEMBRANE PERFORMANCE ANALYSIS

INTRODUCTION

Permeation through polymeric materials is often assumed to occur by the mechanism of activated diffusion. This model assumes that permeation is basically a three step process. First, the permeating molecules dissolve in the polymer. Second, the molecules diffuse through the polymer. Finally, the molecules come out of solution on the downstream side of the polymeric membrane. The diffusion process is believed to depend on the formation of "holes" in the polymeric network, due to thermal agitation of the chain segments*. The diffusional driving force for this mechanism can be shown to be equal to the chemical potential gradient across the membrane**. For an infinitely dilute solution (of permeant in polymer), the chemical potential gradient is proportional to the concentration gradient.

The solubility of the permeating material in the polymer is assumed to follow Henry's Law, i.e., the concentration is proportional to the partial pressure of the permeating molecules. Thus, the driving force for activated diffusion of dilute solution is proportional to the partial pressure difference in the bulk fluid phases on either side of the polymeric membrane. The direction of permeation is, of course, from the high concentration side to the low concentration side.

It is important to note that the activated diffusion model does not differentiate between "liquid" and "gaseous" diffusion. Once the permeating molecules are absorbed in the polymer network, the molecules are neither liquid nor gas; they exist in the polymer solution phase. The permeant concentration in the polymer is a function only of its partial pressure in the bulk fluid phase; thus the partial pressure is the driving force whether the bulk fluid is liquid or gas. In reality, of course, the solubility of the permeating species may be a function of the total pressure as well as the partial pressure. However, the activated diffusion model does not consider these deviations from Henry's Law.

*A. Lebovitz, Modern Plastics, 43, 139 (1966).

**S. B. Tuwiner, Diffusion and Membrane Technology (Reinhold Publishing Corp., New York City, 1962), p. 38.



In accordance with the above description of the activated diffusion model, the overall permeability coefficient π , is defined as the product of the diffusion coefficient of the permeating species in the polymer D , and the solubility of the species in the polymer S , i.e.;

$$\pi = DS \quad (1)$$

The solubility coefficient is related to the Henry's Law constant k by:

$$S = \frac{\rho_m}{k} \quad (2)$$

where ρ_m is the molar density of the polymer.

Experimentally, the determination of the permeability for given conditions does not involve the use of any mechanistic model; the model is important when extrapolation to other conditions is necessary. In the present work, the assumption is made that the permeability of a given species in a particular polymer is constant. The validity of this assumption varies, of course, with the range of conditions and the particular species - polymer system of interest.

Both the diffusivity and the solubility are actually functions of temperature; thus the permeability is also temperature dependent. Fortunately, the diffusivity usually increases and the solubility usually decreases with increasing temperature, thus mitigating the temperature dependence of the permeability. The solubility can vary with concentration and total pressure. The diffusivity can be greatly concentration dependent, especially with water as the permeating species. The water molecules cause "swelling" of the polymer, allowing the diffusivity to increase with concentration*.

Of course, the activated diffusion model may not fully describe the mass transfer. Continuum or rarefied gas flow may be a significant mechanism, depending on the polymer species (and its pore configuration). Some experimenters have found a total pressure driving force for bulk phase liquid permeation**, thus suggesting the predominance of one of the other flow mechanisms. It has been found that oxygen and nitrogen permeation through polymethyl pentene can be predicted quite accurately using equations 1 and 2 as a basis. This statement is based on tests conducted at AiResearch on separating oxygen from nitrogen for fuel tank inerting.

*N. N. Li, R. B. Long, and E. J. Henley, I&EC 57, 18 (1965).
**L. B. Ticknor, J. Phys. Chem 62, 1483 (1958).



The activated diffusion model defines the permeation flux J_i as*

$$J_i = -\pi_i \frac{d\bar{P}_i}{dr} \quad (3)$$

where \bar{P}_i is the partial pressure of component i and r is the diffusing path length (radially through the tube walls). Equation (3) holds for each diffusing component separately. Axial diffusion has been neglected. The effect of the resistance of the bulk fluid phase is neglected since the diffusion rate in the gas phase is many orders of magnitude greater than the diffusion rate in the polymer phase.

Since the interest is in the concentrations on either side of the membrane, Equation (3) can be written

$$J_i = -\pi_i \frac{\Delta \bar{P}_i}{t} = \frac{-\pi_i (\bar{P}_{i_{in}} - \bar{P}_{i_{shell}})}{t} \quad (4)$$

where t is the membrane wall thickness.

The molar flux can be expressed in terms of the flow rate W_i and mass transfer area A ,

$$J_i = \frac{dW_i}{dA} \quad (5)$$

Therefore,

$$dW_i = \frac{\pi_i (\bar{P}_{i_{in}} - \bar{P}_{i_{shell}})}{t} dA \quad (6)$$

Equation (6) can be written for each diffusing component.

*S. B. Tuwiner, Diffusion and Membrane Technology (Reinhold Publishing Corp., New York City, 1962), p. 38.



PERFORMANCE OF TEST UNIT

For simplification, the analysis discussed below assumes the diffusional resistance of the dissolved oxygen in the bulk water is negligible. All the resistance is assumed to occur in the fiber membrane wall. In the following section, where a unit designed to a specific problem statement is evaluated, the diffusional resistance in the bulk fluid will be taken into account.

Since the bulk fluid is in the liquid phase, the bulk density and flow rate will remain relatively constant along the tube. In addition, the permeation rate of water should be small in comparison to the total water flow rate. For these conditions, it is possible to solve Equation (6) analytically. A mass balance can be written over a differential section of a single tube permeant system to yield:

$$(C_{i,out} - C_{i,in}) V \pi R^2 = \frac{-\pi_i (\bar{P}_{i,in} - \bar{P}_{i,shell})}{t} 2\pi R \Delta y \quad (7)$$

where R is the radius of a single tube

Δy is the differential axial length

C_i is the concentration of the diffusing component

V is the bulk fluid velocity, assumed to be constant.

As $\Delta y \rightarrow 0$,

$$V \pi R^2 dC_i = \frac{-\pi_i (\bar{P}_i - \bar{P}_{i,shell})}{t} 2 \pi R dy \quad (8)$$

The concentration can be related to the partial pressure by Henry's Law,

$$C_i = P_i \frac{\rho_{H_2O}}{k} \quad (9)$$

where ρ_{H_2O} is the density of the bulk stream, assumed to be constant,

Equations (8) and (9) can be combined and rearranged to yield,



$$dy = - \frac{VR(\rho_{H_2O})^t}{2k\pi_i} \frac{d\bar{P}_i}{\bar{P}_i - \bar{P}_{i_{shell}}} \quad (10)$$

Equation (10) can be solved to yield

$$\frac{2k\pi_i y}{VR(\rho_{H_2O})^t} = \ln \left[\frac{\bar{P}_i - \bar{P}_{i_{shell}}}{\bar{P}_{i_o} - \bar{P}_{i_{shell}}} \right] \quad (11)$$

Where $\bar{P}_i = \bar{P}_{i_o}$ at $y = 0$

At the outlet, $y = L$, converting to the convenient log mean partial pressure difference defined as

$$\Delta\bar{P}_{i_{lm}} = \frac{(\bar{P}_{i_L} - \bar{P}_{i_{shell}}) - (\bar{P}_{i_o} - \bar{P}_{i_{shell}})}{\ln \left[\frac{\bar{P}_{i_L} - \bar{P}_{i_{shell}}}{\bar{P}_{i_o} - \bar{P}_{i_{shell}}} \right]} \quad (12)$$

simplifies to

$$\Delta\bar{P}_{i_{lm}} = (\bar{P}_{i_L} - \bar{P}_{i_o}) \left(\frac{VR(\rho_{H_2O})^t}{2k\pi_i L} \right) \quad (13)$$

Combining Equation (13) with Equation (9) yields

$$\Delta\bar{P}_{i_{lm}} = (c_{i_L} - c_{i_o}) \frac{VRt}{2\pi_i L} \quad (14)$$

Since the velocity is constant, the permeant flow rate is given by

$$W_i = (c_{i_L} - c_{i_o}) V\pi R^2 \quad (15)$$

so that

$$\Delta\bar{P}_{i_{lm}} = \frac{W_i t}{2\pi RL \pi_i} \quad (16)$$



But $2\pi RL$ is simply the mass transfer area of a single fiber. Since the permeant flows from each of the tubes are additive, the total permeant flow rate is

$$W_i = \frac{A_{\pi_i}}{t} \Delta \bar{P}_{i_{lm}} \quad (17)$$

The tube side pressure drop can be determined from the Hagen-Poiseuille equation for laminar, incompressible flow in circular tubes,

$$\Delta P = \frac{32\mu L_w}{(\rho_{H_2O}) A_f g_c D^2} \quad (18)$$

where A_f is the total flow area.

Using the value for the permeability of oxygen through polymethyl pentene shown in Table 2-1, it was found that the laboratory unit had the capacity of decreasing the dissolved oxygen partial pressure from 50 to 3 psia at a water rate flow rate of 160 lb/hr. As noted previously, the maximum pressure drop across the tube sheet of the laboratory test unit is limited to 17 psi, this resulted in maximum flow rate of about 26 lb/hr. Thus, the oxygen partial pressure of the deaerated water would be expected to be very close to the shell side oxygen partial pressure. As shown in Table 2-3 this did occur for all three types of shell side conditions.



FLIGHT UNIT

The design condition, in this task order, was for a deaerator to be used to obtain a hard fill of the expendable EVLSS water tank during servicing. The problem statement is given in Table 3-1; shell side pressure was assumed to be space vacuum (effectively zero). For this preliminary design, the effect of diffusional resistance in the bulk liquid was included in determining the overall performance of the unit.

TABLE 3-1

DEAERATOR PROBLEM STATEMENT

Water Flow Rate	54 lb/hr
Water Pressure	50 psia
Water Temperature	40 to 90°F
Water Side ΔP	5 psi
Dissolved Gas	
In	Saturated with nitrogen at 50 psia
Out	Saturated with nitrogen at 3 psia (max)

To determine the effect of bulk phase diffusion, consider an incompressible fluid flowing through a circular tube in the laminar regime. If the total density is constant, a mass balance performed on a cylindrical shell of the fluid yields*

$$\left(v_x\right)\frac{\partial c_a}{\partial x} + \left(v_r\right)\frac{\partial c_a}{\partial r} = D_{ab} \left[\frac{1}{r} \frac{\partial}{\partial r} \left(r \frac{\partial c_a}{\partial r} \right) + \frac{\partial^2 c_a}{\partial x^2} \right] \quad (19)$$

where V is the velocity and

C_a is the concentration of the diffusing component

x and r are the axial and radial directions

D_{ab} is the diffusivity of component "a" in the bulk phase "b",

*W. M. Rohsenow and H. Y. Choi, Heat, Mass and Momentum Transfer (Prentice-Hall, Inc., Englewood Cliffs, N.J. 1961), p. 401.



Equation (19) is simply Fick's first law of diffusion written in cylindrical coordinates. If the flow is fully developed, $V_r = 0$. For negligible axial diffusion, $(V_x) \frac{\partial C_a}{\partial x} \gg D_{ab} \frac{\partial^2 C_a}{\partial x^2}$ so Equation (22) reduces to

$$(V_x) \frac{\partial C_a}{\partial x} = D_{ab} \left[\frac{1}{r} \frac{\partial}{\partial r} \left(r \frac{\partial C_a}{\partial r} \right) \right] \quad (20)$$

The solution of Equation (20) involves the assumption of a functional form for the fluid velocity V_x and the assignment of boundary conditions. For "undisturbed" laminar flow, the velocity profile is parabolic, i.e.,

$$V_x = 2V \left[1 - \left(\frac{r}{R} \right)^2 \right] \quad (21)$$

where V is the bulk average velocity.

For the boundary condition of constant concentration at the wall ($r = R$), Equations (20) and (21) have been solved. The asymptotic solution for large $\frac{x}{R}$ yields the familiar limiting Nusselt number for a fully developed concentration profile*. There are also solutions for constant flux at the wall**. Unfortunately, neither of the above boundary conditions is applicable to the present problem.

The boundary conditions here are that the flux at the permeant wall is proportional to the concentration difference across the wall. In his treatise on solutions to differential equations applicable to mass transfer problems, Crank*** presents a solution for non-steady state diffusion in a solid cylinder with surface evaporation which is useful for the present problem. Crank solves the equation

$$\frac{\partial C_a}{\partial \theta} = D_{ab} \left[\frac{1}{r} \frac{\partial}{\partial r} \left(r \frac{\partial C_a}{\partial r} \right) \right] \quad (22)$$

with the boundary condition

$$-D_{ab} \frac{\partial C_a}{\partial r} = \alpha (C_a - C_w) \text{ at } r = R \quad (23)$$

where θ is time

and α and C_w are constants

*For the identical heat transfer solution see, e.g., M. Jakob, Heat Transfer, Vol. I (John Wiley and Sons, Inc. New York City, 1949), p. 451.

**C. O. Bennett and J. E. Myers, Momentum, Heat, and Mass Transfer (McGraw Hill Book Company, Inc. New York City, 1962), p. 308.

***J. Crank, The Mathematics of Diffusion (Oxford University Press, London, 1956), p. 13



Equation (22) is identical to Equation (20) for

$$\theta = \frac{x}{V_x} \quad (24)$$

with V_x constant. The boundary condition given in Equation (23) is directly applicable to the present problem for which the flux at the wall is proportional to the concentration difference across the wall, i.e.,

$$-D_{ab} \frac{\partial C}{\partial r} = \frac{\pi}{tS} (C_a - C_w) \text{ at } r = R \quad (25)$$

For the deaerator, $C_w = 0$. Crank's solution is for a uniform rather than parabolic velocity profile. A strictly uniform velocity profile is, of course, a physical impossibility since it is equivalent to perfect slip at the wall. There is some evidence that the mass transfer through the wall may reduce the skin function and hence promote slip flow at the wall*. In any event, a mass transfer "margin" is incorporated in the design in case the uniform velocity profile solution overestimates the actual performance.

The solution given in Crank** is

$$\frac{C_o - C_a}{C_o} = 1 - \sum_{n=1}^{\infty} \frac{2MJ_o\left(\frac{r}{R}\beta_n\right)}{(\beta_n^2 + M^2)J_o(\beta_n)} e^{-\left(\frac{\beta_n^2 D_{ab}}{V_x R^2} x\right)} \quad (26)$$

where the J 's are Bessel functions of the first kind

C_o is the concentration of component "a" entering the unit and

$$M = \frac{R\pi}{tS D_{ab}} \quad (27)$$

and the β_n 's are the roots of $\beta_n J_1(\beta_n) - M J_0(\beta_n) = 0$.

For a given unit, Equation (26) predicts the concentration of the diffusing component at any axial and radial position. It is perhaps of greater interest to consider the bulk or mixing-cup concentration C_m at a given axial location defined by***.

*J. M. Kay, Aeronautical Research Council, R&M, No. 2628, 1953.

**J. Crank, The Mathematics of Diffusion (Oxford University Press, London, 1956), p. 73.

***W. M. Rohsenow and H. Y. Choi, Heat, Mass, and Momentum, P. 308



REPRODUCIBILITY OF THE
ORIGINAL PAGE IS POOR

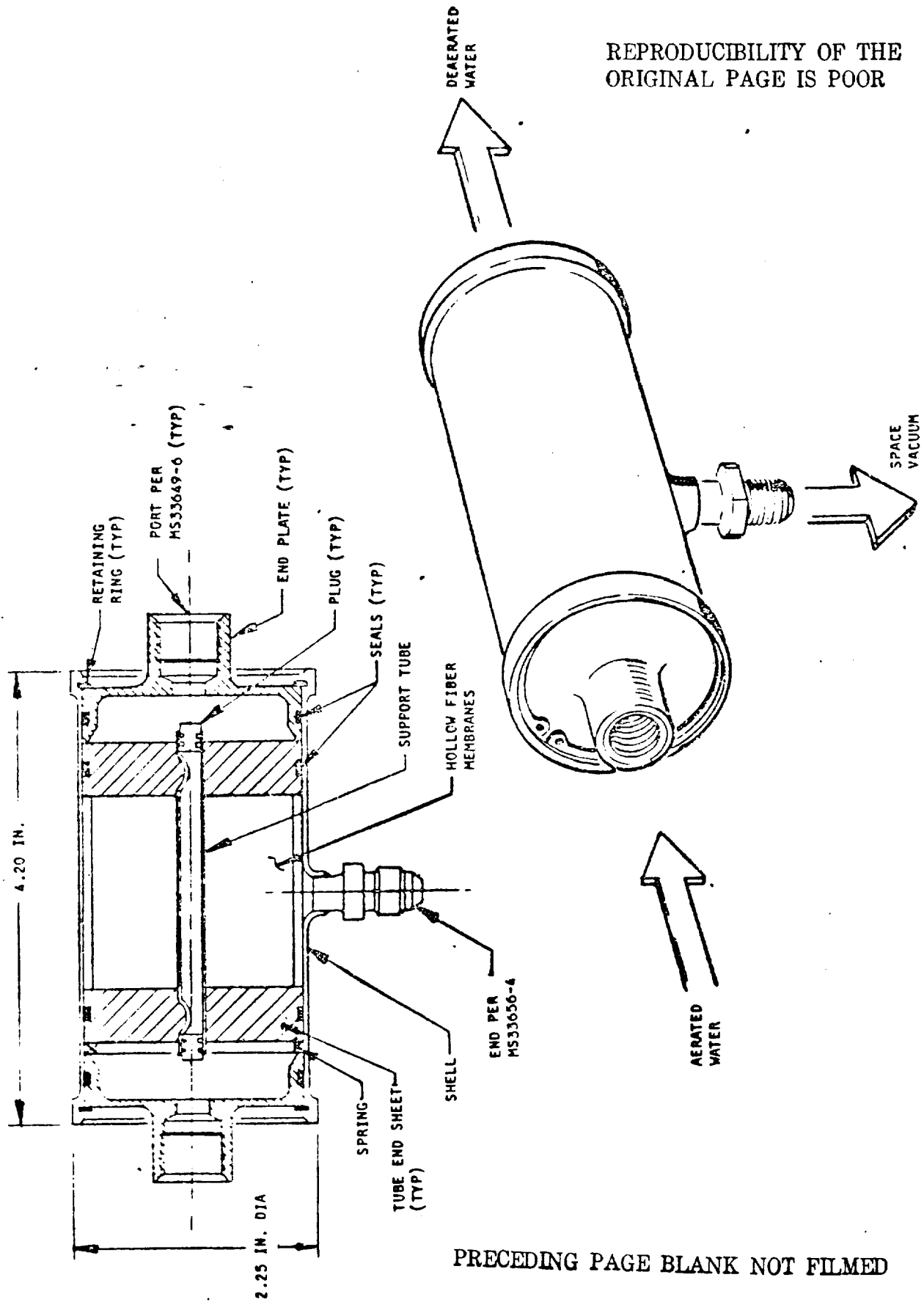


Figure 3-1. Water Deaerator

PRECEDING PAGE BLANK NOT FILMED



AIRSEARCH MANUFACTURING COMPANY
OF CALIFORNIA

REPRODUCIBILITY OF THE
ORIGINAL PAGE IS POOR

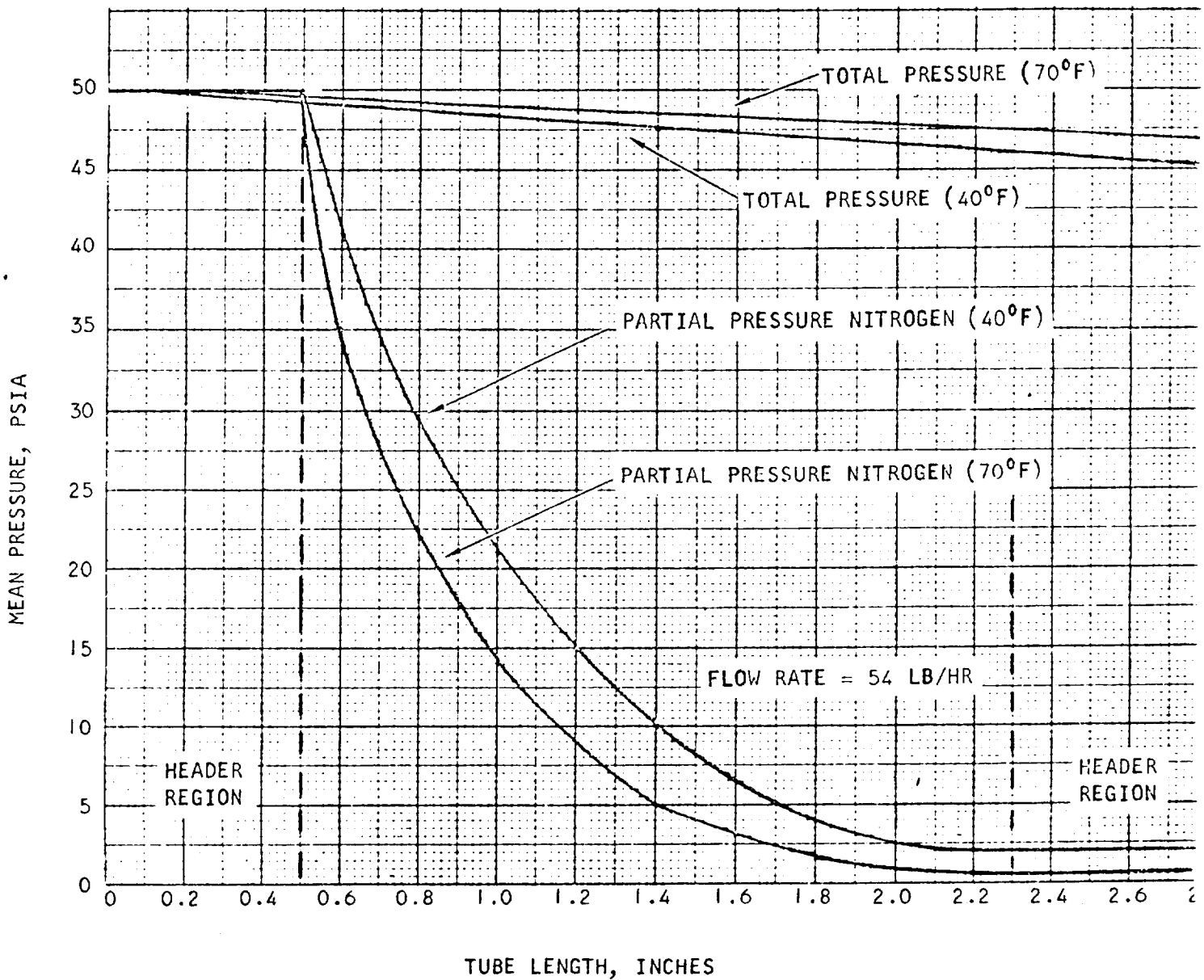


Figure 3-2. Predicted Performance of Flight Unit



The total pressures are also shown in Figure 3-2. There may be some nitrogen coming out of solution in the inlet header region.

In Figure 3-3, the predicted outlet mixing-cup partial pressures are shown for various bulk flow rates at 40°F.

The water permeation rate is very small, 3.6×10^{-3} lb/hr at 40°F. For the design conditions of 40°F and 54 lb/hr, bulk flow rate, the nitrogen permeation rate is 4.6×10^{-3} lb/hr. Water loss in the unit, permeation through the fiber walls is therefore negligible.



REPRODUCIBILITY OF THE
ORIGINAL PAGE IS POOR

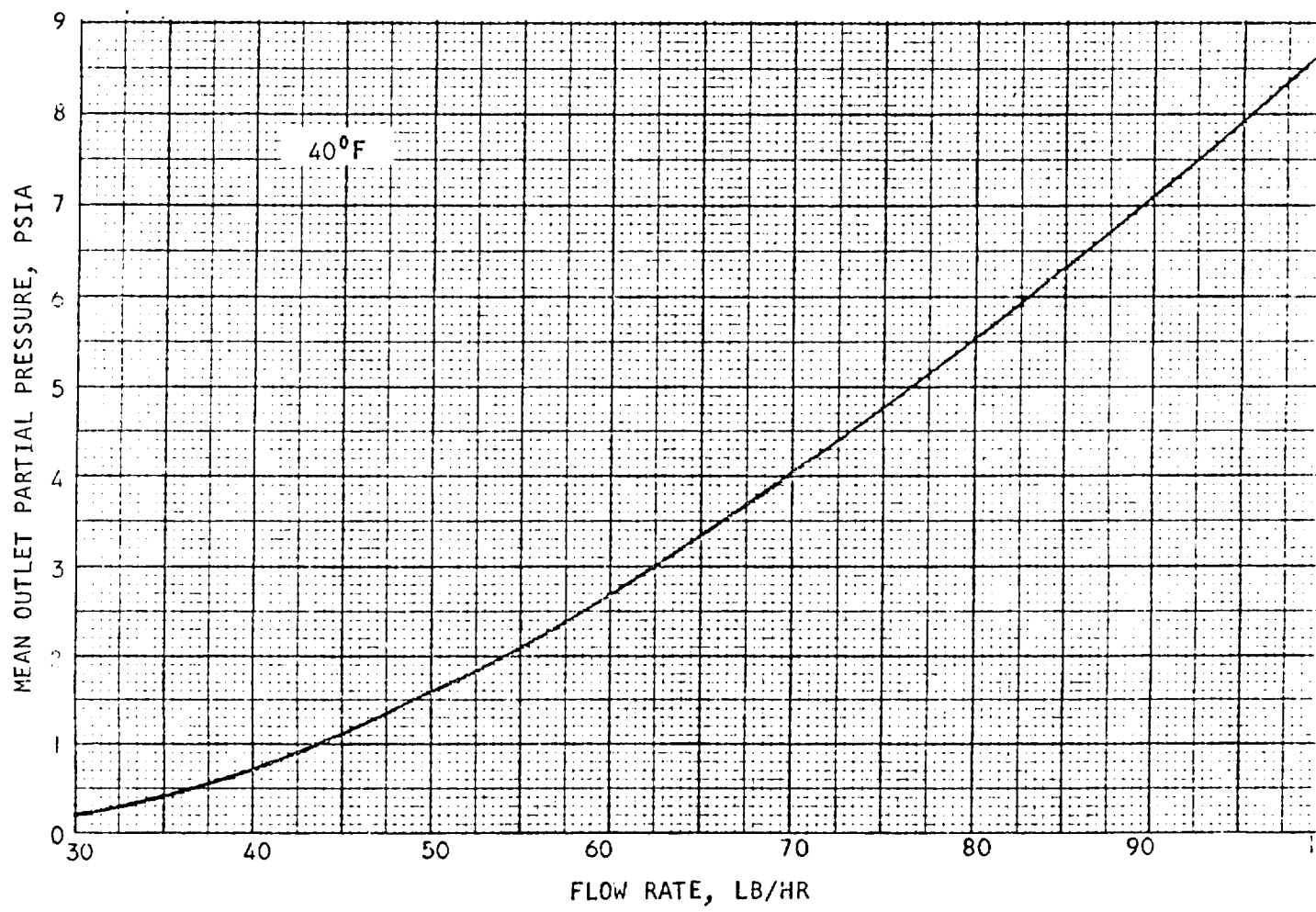


Figure 3-3. Effect of Flow Rate



